Published as: Dan Matlhomola Molefe, FJWJ (Johan) Labuschagne, Walter W Focke, Isbé van der Westhuizen and Osei Ofosu. Magnesium hydroxide derivatives as fire retardants for plasticized PVC. Journal of Fire Sciences November 2015 vol. 33 no. 6 493-510 doi: 10.1177/0734904115612501 http://jfs.sagepub.com/content/33/6/493.abstract

The effect of magnesium hydroxide, hydromagnesite and layered double hydroxide on the heat stability and fire performance of plasticized poly(vinyl chloride)

Dan Matlhomola Molefe[1], FJWJ (Johan) Labuschagne[2], Walter W Focke[2,*], Isbé van der Westhuizen[2] and Osei Ofosu[3]

[1]Department of Chemistry, University of Pretoria, Private Bag X20, Hatfield 0028, South Africa

[2]Institute of Applied Materials, Department of Chemical Engineering, University of Pretoria, Private Bag X20, Hatfield 0028, South Africa

[3]CSIR Materials Science and Manufacturing, PO Box 1124, Port Elizabeth 6000, South Africa

Details of the authors are as follows:

Dan Matlhomola Molefe (Dan.Molefe@up.ac.za) Tel. + 27 82 202 2095

Department of Chemistry, University of Pretoria, Private Bag X20, Hatfiels 0028, Pretoria, South Africa

Dan is a senior lecturer in the Department of Chemistry, University of Pretoria. He is also a PhD student supervised by Dr Labushagne and Prof Focke.

FJWJ (Johan) Labuschagne (Johan.Labuschagne@up.ac.za) + 27 83 307 4544

Institute of Applied Materials, Department of Chemical Engineering, University of Pretoria, Private Bag X20, Hatfield 0028, Pretoria, South Africa

He is a senior lecturer in the Department of Chemical Engineering, University of Pretoria. His research interests include polymer additives, with a particular focus on layered double hydroxides.

Walter Wilhelm Focke (walter.focke@up.ac.za) Tel +27 83 326 6549

Institute of Applied Materials, Department of Chemical Engineering, University of Pretoria, Private Bag X20, Hatfield 0028, Pretoria, South Africa

Walter Focke obtained a MEng degree in Chemical Engineering from the University of Pretoria and a PhD in Materials Science and Engineering from MIT. He is the director of the Institute of Applied Materials at the

University of Pretoria. His research interests include polymer additives, clay nanotechnology, pyrotechnics, and malaria vector control.

Isbé van der Westhuizen (Isbe.Vanderwesthuizen@up.ac.za) +27 82 298 8653
Institute of Applied Materials, Department of Chemical Engineering, University of Pretoria, Private Bag X20, Hatfield 0028, Pretoria, South Africa

She is a thermal analysis specialist working in the Institute of Applied Materials.

Osei Ofosu (oofosu@csir.co.za) holds an MSc in Materials Engineering from the University of Cape Town and is a research engineer at the CSIR in Port Elizabeth. His research interest include development, characterization and cone calorimeter testing of novel natural fibre reinforced composites for automotive and aerospace applications.

Acknowledgements

Financial support (via Grants P2010072800070 and TP13080124921 "Beneficiation of hydrotalcite") from the THRIP programme of the Department of Trade and Industry and the National Research Foundation as well as Greenfield Innovation and Blue Sky Venture Partners is gratefully acknowledged.

Abstract

Emulsion grade PVC was plasticised with 100 phr diisononyl phthalate and filled with 30 phr of different hydrated filler-type flame retardant additives. Static heat stabilities were determined at 200 °C by following the time dependence of hydrogen chloride evolution. Fire retardant performance was studied with a cone calorimeter at a radiant flux of 35 kW m^{-2}. The layered double hydroxide outperformed the other fillers with regard to improving static heat stability and also with respect to most fire retardant performance indices.

Keywords

Layered double hydroxide; poly(vinyl chloride); heat stabiliser; thermal analysis

Introduction

Magnesium hydroxide [$Mg(OH)_2$] (MH) occurs in nature as the mineral brucite. It has a layered structure composed of stacked trioctahedral metal hydroxide sheets. Hydrotalcite is a natural anionic clay mineral [$Mg_6Al_2(OH)_{16}CO_3.4H_2O$]. Layered double hydroxides (LDHs) are synthetic analogues (1-3). LDHs also feature the stacked sheet structure of brucite (3). The difference is that a portion of the magnesium ions in the sheets have been replaced with aluminium ions. This substitution imparts a net positive charge that is balanced by an equal negative charge from the interlayer carbonate anions. Water molecules also occupy the interlayer space. Hydromagnesite [$4MgCO_3.Mg(OH)_2 \cdot 4H_2O$] (HM) is a basic magnesium hydroxycarbonate mineral that also has a layered structure (4).

PVC is a very versatile polymer with diverse applications. Neat PVC features a relatively high chlorine content of 56.7 wt.%. That makes it more resistant to ignition and burning than most organic polymers (5). Furthermore, pyrolysis of PVC yields an isotropic carbon char residue (6) and this contributes to the mechanisms of flame retardant action (7). However, the conventional plasticizers used in the manufacture of flexible PVC detract from this outstanding fire resistance. Therefore, flame-retardant (FR) and smoke-suppressant (SS) additives must be incorporated in order to meet product test specifications such as oxygen index, heat release rate, smoke evolution, etc. (5).

Levchik and Weil (8) and Weil *et al*. (9) reviewed the chemical additives that have been considered to achieve acceptable fire properties in the principal PVC application areas. The hydrated filler additives aluminium trihydrate, magnesium hydroxide (MH), hydromagnesite (HM) and layered double hydroxide (LDH) have utility as endothermic flame retardants and smoke suppressants for PVC as well as other polymers (10-14). Their flame retardant action relies on endothermic decomposition reactions that absorb heat and release inert gases, e.g. steam and carbon dioxide (11, 15, 16). The cooling of the polymer

substrate inhibits solid phase decomposition reactions. Simultaneously the steam and/or carbon dioxide released by the decomposition reactions dilutes the surrounding atmosphere with an inert gas. Finally, the residues may form an ash-char barrier layer at the surface that reduces heat transfer from the flame to the remaining polymer substrate.

Neat PVC is thermally unstable (17) and prone to autocatalytic dehydrochlorination (18). The hydrogen chloride assumes a catalytic role in the degradation mechanism (19). In practice the thermal instability associated with the use of PVC is overcome through the use of heat stabilizer additives.(17) Scavenging the liberated HCl generated by the degradation reaction is one way to retard the degradation. Layered double hydroxides (LDHs) provide heat stabilization to PVC owing to their intrinsically high capacity to react with HCl (20-24). The thermal stabilisation action of LDH involves two steps. Initially, HCl formed during thermal dehydrochlorination, displaces the carbonate interlayer anions to afford LDHs with Cl^- anions in the interlayer. As further dehydrochlorination takes place, the HCl reacts with the clay itself, ultimately destroying its structure and forming metal chlorides, metal hydroxy-chlorides and hydrates of $MgCl_2$ and $AlCl_3$ (21).

This communication reports on the performance of magnesium hydroxide, hydromagnesite and LDH on the thermal stability, fire retardancy and smoke suppression of plasticized PVC. Static heat stability was determined using the Thermomat technique and fire performance was determined with a cone calorimeter. The objective was to determine whether LDH-based heat stabilizer can impart fire retardant properties comparable to those provided by magnesium hydroxide and hydromagnesite.

Experimental

Materials

Reagent grade (95%) magnesium hydroxide and magnesium oxide (light, 95%) was obtained from Sigma-Aldrich. Industrial grades magnesium oxide and $Al(OH)_3$ were supplied by Chamotte Holdings. All other chemicals were analytical grade reagents supplied by Merck. TPC Paste Resin Co., Ltd. supplied PG680, an emulsion grade poly(vinyl chloride). It was a free flowing powder with a K-value of 69. The diisononyl phthalate (DINP) plasticiser was supplied by Isegen.

Synthesis of LDH and hydromagnesite. The layered double hydroxide (LDH) $[Mg_{0.667}Al_{0.333}(OH)_2](CO_3)_{0.167}.mH_2O]$ was synthesised according to the method described by Labuschagné *et al*. (25). The procedure was as follows: The $Al(OH)_3$ and light MgO powders were mixed in the required 2:1 stoichiometric ratio. The powder mix was slowly added, while stirring, to one litre of distilled water in a 1.6 L Parr autoclave. The final solids concentration of the slurry was 15 wt. %. A 60 mol % excess of $NaHCO_3$ was added to the mixture as the source for the intercalate anion. The reaction was conducted under vigorous stirring at a temperature of 180 °C and a pressure of approximately 14 bar. The autoclave was kept at this temperature and pressure for approximately 5 h. Thereafter heating was discontinued and the reaction mixture was allowed to cool overnight while stirring. The solid product was removed from the autoclave, filtered and washed several times with distilled water to remove residual Na_2CO_3. Finally it was dried in an oven at 80 °C for at least 48 h.

The hydromagnesite was also synthesized according to the method described by Labuschagné *et al*. (25) as follows. Magnesium oxide stock from Chamotte Holdings was calcined at 800 °C for 10 min. A total of 100 g of the cooled MgO was suspended in 1.5 L distilled water using a Silverson disperser at 6700 rpm. An ice bath was used to keep the temperature of the mixture at approximately 23 °C. Carbon dioxide was bubbled through the

mixture to form hydromagnesite. The pH gradually dropped and stabilised at 8.2. It was maintained at this value for another 30 min. The mixture was filtered and the precipitate dried in an oven at 140 °C for approximately 12 h. Finally the dry sample was ground to a fine powder.

Surface coating of the fillers. All samples were coated with stearic acid as follows: The dried solids were milled to a fine powder using a coffee grinder. They were then suspended in 1 L distilled water and heated to 75 °C. The solids content of all the slurries was less than 20 wt. %. The slurries were vigorously agitated with a Silverson disperser. Stearic acid, equivalent to 2.0 wt. % based on the total dry uncoated solid sample, was added to the hot slurry. The suspension was stirred for 15 min at 6000 rpm. The coated powders were recovered by filtering. They were dried in a convection oven set at 60 °C and ground to a fine powder.

Preparation of PVC-composites. DINP plasticiser (130 g) was weighed into a 600 mL beaker. Next small portions of the PVC powder (up to a total of 130 g) were added and mixed using a high-speed Anvil milkshake mixer. The dispersion was de-aerated for about 30 minutes in a Speedvac vacuum chamber. Then the LDH filler powder (39 g) was incorporated. The dispersion was again de-aerated but this time for about 1 h.

Cast PVC composite sheets were made in a three-step pressing process. The paste mixture was poured into a mould measuring 100 mm × 100 mm × 3.5 mm. The mould was closed and placed in convection oven set at a temperature of 130 °C for 10 minutes. Then it was hot pressed at a pressure of 10 MPa at 150 °C for 5 min. The mould was then removed from the press and a heavy weight placed on the top plate. The moulding was allowed to cool down at ambient conditions before it was removed.

Material characterisation

Where applicable, uncertainties indicated in measured values correspond to one standard deviation.

Particle size and BET surface area determination. The particle size distributions were determined with a Mastersizer Hydrosizer 2000MY (Malvern Instruments, Malvern, UK). The specific surface areas of the powders were measured on a Nova 1000e BET instrument in N_2 at 77 K.

Scanning Electron Microscopy (SEM). A small quantity of powder was placed onto carbon tape on a metal sample holder. Excess powder was removed using a single compressed air blast. The samples were then coated five times with carbon under argon gas using the Polaron Equipment E5200 SEM auto-coating sputter system. The powder samples were viewed on a Zeiss Ultra plus FEG SEM scanning electron microscope.

X-ray diffraction (XRD). X-ray diffraction analysis was performed on a PANalytical X-pert Pro powder diffractometer fitted with an X'celerator detector using Fe filtered CoKα radiation (0.17901 nm). The instrument featured variable divergence and receiving slits. X'Pert High Score Plus software was used for data manipulation and phase identification.

X-ray fluorescence (XRF). Chemical composition was determined by the X-ray fluorescence method. Milled samples (< 75 μm) of the materials were roasted at 1000 °C for at least 3 hours to oxidize Fe^{2+}. Glass disks were prepared by fusing 1 g roasted sample and 8 g of a flux (consisting of 35% $LiBO_2$ and 64.71% $Li_2B_4O_7$) at 1050 °C. The glass disks were analyzed by a PANalytical Axios X-ray fluorescence spectrometer equipped with a 4 kW Rh tube.

Inductively coupled plasma optical emission spectrometry (ICP-OES). The elemental composition of the LDH was determined with a Spectro Arcos model inductively coupled plasma optical emission spectrometer (ICP-OES). First about 0.5 g of the clay was dissolved

in 50 mL Aqua Regia. After cooling down, the reaction mixture was diluted with 50 mL of distilled water and filtered through ashless filter paper. Before performing the ICP-OES analysis, 1 mL of solution was added to 99 mL of distilled water. The analysis was then performed, analysing for copper, magnesium, aluminium, calcium, zinc, iron and sodium. The insoluble fraction was determined by ashing the filter paper.

Fourier transform infrared spectroscopy (FTIR). FTIR spectra were recorded on a PerkinElmer 100 Spectrophotometer. Powder samples were pressed onto the Zn/Se plate of a MIRacle ATR attachment. The spectra were obtained over the range 650 – 4000 cm^{-1} and represent the average of 32 scans at a resolution of 2 cm^{-1}.

Thermogravimetric Analysis (TGA). Thermogravimetric analysis (TGA) was performed using the dynamic method on a Mettler Toledo A851 TGA/SDTA instrument. About 11-15 mg sample was placed in an open 150 µL alumina pan. Temperature was scanned from 25 °C to 900 °C at a scan rate of 10 °C min^{-1} with air or nitrogen flowing at a rate of 50 mL min^{-1}.

Heat stability assessment

The heat stability of the PVC compounds was evaluated on a Metrohm 895 Professional PVC Thermomat according to ISO 182 Part 3 (26). The method is based on the fact that PVC releases HCl when it decomposes at high temperatures. The evolved hydrochloric acid is flushed with a stream of nitrogen gas and passed through a measuring vessel where it is absorbed in purified water. The progress of the decomposition is tracked by measuring the change in the conductivity of this water. Performance is quantified in terms of either the induction time (i.e. the time that is required to reach the break point in the conductivity curve) or a stability time, i.e. the time until a conductivity difference of 50 µS cm^{-1} is reached. The PVC compound sample amount tested was 0.50 ± 0.05 g. The samples were

cut into small pieces less than 1 mm in size. The stability was determined in duplicate at 200 °C. Nitrogen flow was controlled at 7 L h^{-1} and 50 mL deionised water was used to trap the HCl.

Cone calorimeter fire testing

The ISO 5660 standards (27-29) were followed in performing the cone calorimeter tests using a Dual Cone Calorimeter (Fire Testing Technology (UK) Ltd.). Three specimens of each composition were tested. The sheet dimensions were 100 mm × 100 mm × 3.5 mm with uncertainty of ± 0.1 mm in all dimension measurement. They were placed on aluminium foil and exposed horizontally to an external heat flux of 35 kW m^{-2}. This heat flux was chosen on the basis of the study conducted by Wang *et al*. (30). They studied 3 mm to 10 mm thick PVC sheets at heat fluxes of 25, 35 and 50 kW m^{-2}. They found that the time to ignition varied linearly with the inverse of the cone calorimeter heat flux. Furthermore, the minimum heat flux for ignition of sheets in this thickness range was found to be about 19 kW m^{-2}. The smoke photometer used a helium-neon (He-Ne) laser that emits red light with a wavelength of 632.8 nm.

Results

Characterization of the hydrated fillers

Figure 1 shows FEG SEM micrographs of the hydrated filler powders. The individual powder particles are made up of highly agglomerated flake-shaped crystals. The primary flakes were smallest for the LDH and largest for the hydromagnesite. Table 1 reports the particle sizes and the BET specific surface areas for the filler additives. The median (d_{50}) particle size

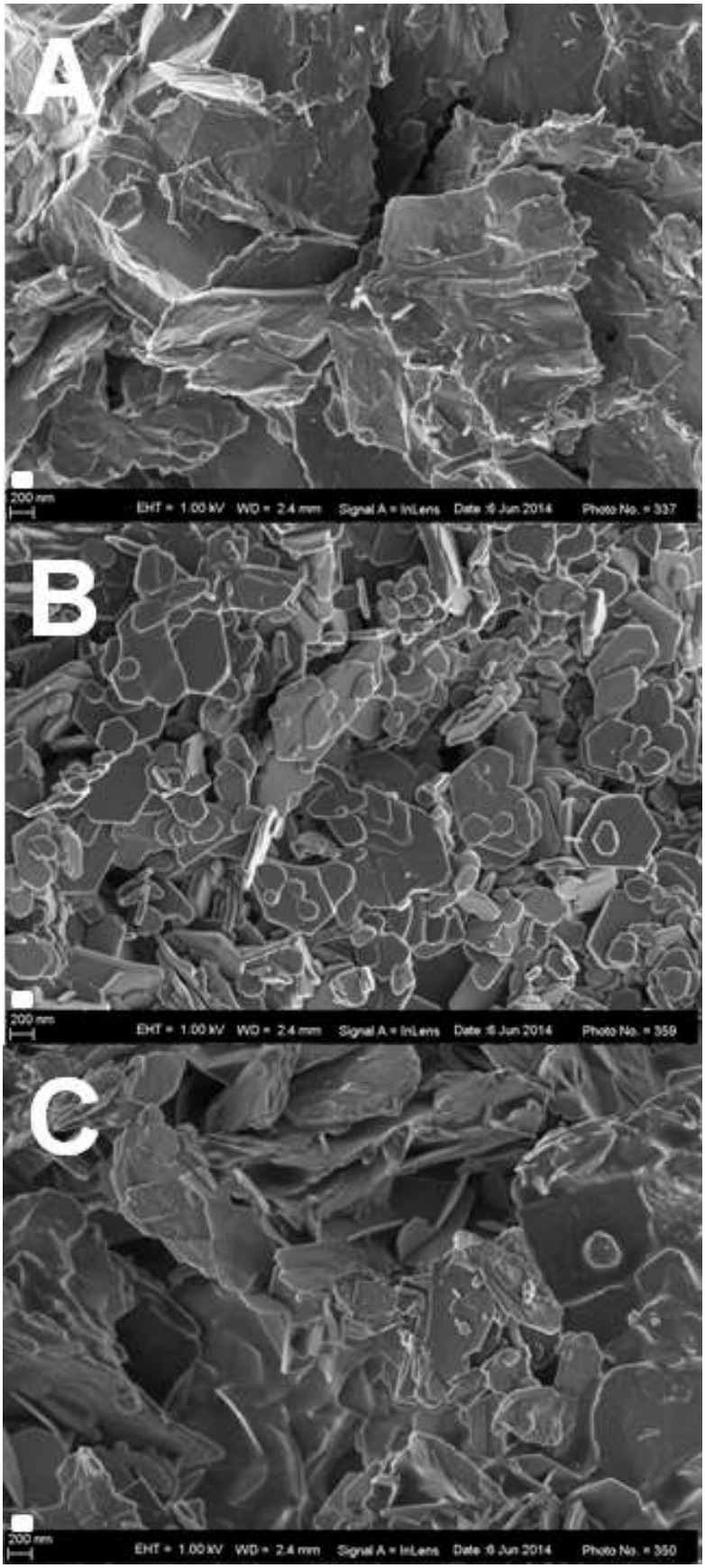

Figure 1. SEM micrographs of (A) Hydromagnesite (HM); (B) Layered double hydroxide (LDH); and (C) Magnesium hydroxide (MH). The size bar indicates a length of 200 nm.

Table 1. LDH particle sizes, BET surface area and d-spacing from XRD results

	Surface area	**d-spacing**	**Particle size, μm**		
Sample	$m^2\ g^{-1}$	nm	d_{10}	d_{50}	d_{90}
MgAl-LDH	18.3	0.761	0.68 ± 0.00	3.08 ± 0.03	13.1 ± 0.3
$Mg(OH)_2$	9.4	0.478	0.93 ± 0.01	3.78 ± 0.12	43.2 ± 2.4
Hydromagnesite	24.8	0.924	2.96 ± 0.08	9.75 ± 0.16	29.7 ± 1.5

varied from 3.1 μm to 9.8 μm. BET surface was highest for the hydromagnesite (24.8 $m^2\ g^{-1}$) and lowest for the magnesium hydroxide (9.4 $m^2\ g^{-1}$).

Table 2 shows the chemical composition data obtained for the various samples. The XRF chemical composition results for the LDH, expressed in terms of the general formula $[Mg_{2+\alpha}Al_{1-\alpha}(OH)_6](CO_3)_{(1-\alpha)/2}\cdot xH_2O$, indicated an apparent α value of 0.025. The magnesium hydroxide contained aluminium and silica as impurities. The other samples contained, in addition, minor amounts of iron, manganese nickel and calcium as impurities.

Table 2. XRF composition analysis data of samples roasted at 1000 °C

Concentration, wt.%	SiO_2	Al_2O_3	Fe_2O_3	MnO	MgO	CaO	NiO
MgAl-LDH	1.59	36.85	0.15	0.00	60.51	0.72	0.18
Hydromagnesite	3.53	0.19	0.21	0.07	94.92	0.89	0.18
$Mg(OH)_2$	0.54	0.30	0.00	0.00	99.16	0.00	0.00
MgO	7.89	0.79	0.80	0.03	89.38	0.92	0.18
Std dev (%)	0.04	0.30	0.15	0.00	60.51	0.72	0.18

X-ray diffraction (XRD). The XRD patterns for the hydrated fillers are shown in Figure 2. The reflections at 2θ = 13.474° and 2θ = 27.125° in the XRD diffractogram for LDH are consistent with a brucite layer basal spacing of 0.761 nm. The d-spacing values for the other compounds are listed in Table 1. It was larger (0.924 nm) for the hydromagnesite and lower (0.478 nm) for the $Mg(OH)_2$. There are additional reflections appearing in the XRD spectrum for the hydromagnesite indicating the presence of impurity phases dypingite

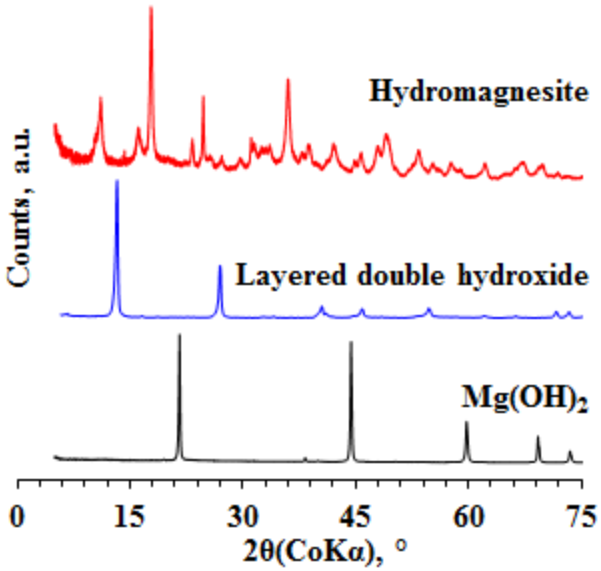

Figure 2. X-ray diffraction patterns for magnesium hydroxide (MH), hydromagnesite (HM) and layered double hydroxide (LDH).

$[Mg_5(CO_3)_4(OH)_2 \cdot 5H_2O]$ and magnesite [MgO]. The sharp nature of the reflections points to a high crystallinity of the corresponding powders.

Fourier transform infrared spectroscopy (FTIR). The $Mg(OH)_2$ spectrum shown in Figure 3 is characterized by a sharp and intense –OH stretching vibration peak at ca. 3700

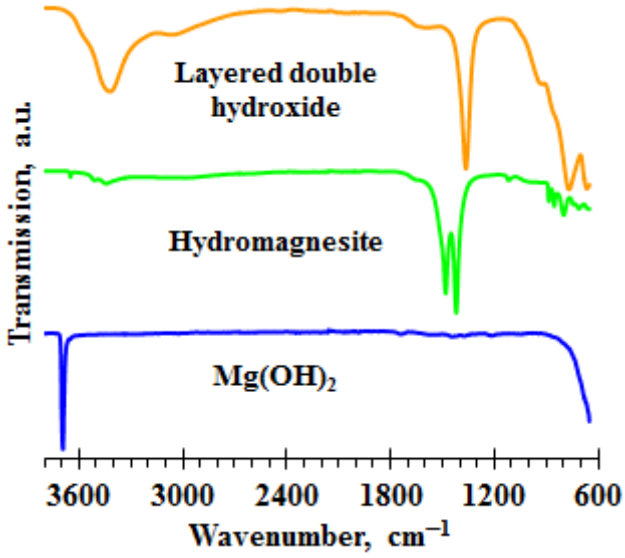

Figure 3. FTIR spectra of the hydrated fillers.

cm^{-1}. This peak is also observed in the hydromagnesite but in the LDH it is much broader and it is centred at a lower wavenumber (ca. 3450 cm^{-1}). It is attributed to –OH stretching vibrations in the octahedral layer and the free and hydrogen bonded water molecules present in the interlayer. The shoulder observed at 3000 cm^{-1} for LDH arises from interactions between carbonate (CO_3^{2-}) and H_2O in the interlayer region (31). The LDH features a single carbonate peak at 1367 cm^{-1} while in the hydromagnesite the carbonate asymmetric stretching vibration band is split with peaks at 1420 cm^{-1} and 1480 cm^{-1}. The latter also features a carbonate symmetric stretch band at ca. 1120 cm^{-1} and three bending bands at 800 cm^{-1}. The presence of the water of crystallization is indicated by the bands at ca. 3510 cm^{-1} and 3450 cm^{-1} (4).

Thermogravimetric analysis (TGA). Figure 4 summarises the TGA mass loss curves for the LDH, magnesium hydroxide and hydromagnesite samples as obtained in an air atmosphere. The nature of the degradation steps for these three compounds were elucidated in previous studies (32-37). In each case water, or water and carbon dioxide are released in

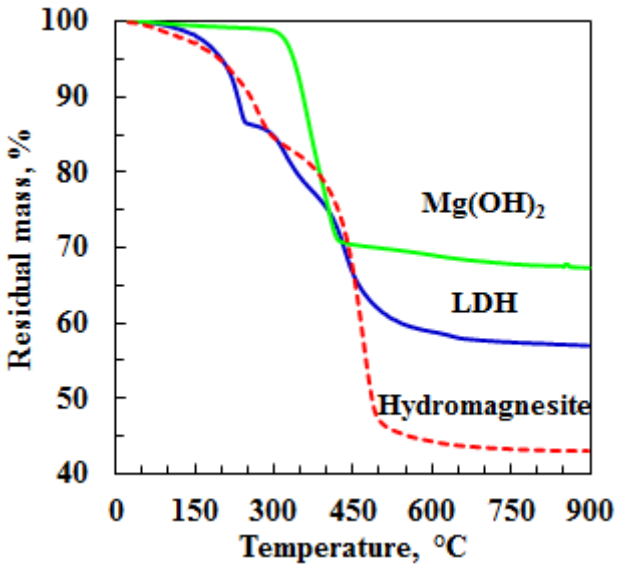

Figure 4. TGA traces in air for the hydrated fillers. Temperature was scanned from 25 °C to 900 °C at a scan rate of 10 °C min^{-1} with air flowing at a rate of 50 mL min^{-1}.

gaseous form and inert oxides remain. The residual masses at the 900 °C were 67.3 wt.%, 56.8 wt.% and 43.1 wt.% for $Mg(OH)_2$, hydrotalcite and hydromagnesite respectively. The corresponding theoretically expected values are 69.1 wt.%, 56.1 wt.% and 43.1 wt.% for $Mg(OH)_2$, hydrotalcite and hydromagnesite respectively. The small discrepancies are attributed to the presence of the indicated impurities and slight deviations from the idealized compositions of the fillers.

Characterisation of the PVC composites

Figure 5 shows TGA traces for the LDH-PVC compounds recorded in air and in nitrogen atmospheres. In nitrogen atmosphere the flexible PVC apparently suffers major mass loss in two main steps. The first stage commences at 240 °C, reaches a maximum rate at 315 °C and ends at 370 °C. At this point the residue is 20.7 wt. %. The second stage starts as 420 °C reaches a maximum rate at 467 °C and ends at 510 °C with a residue of 7.0 wt. % remaining.

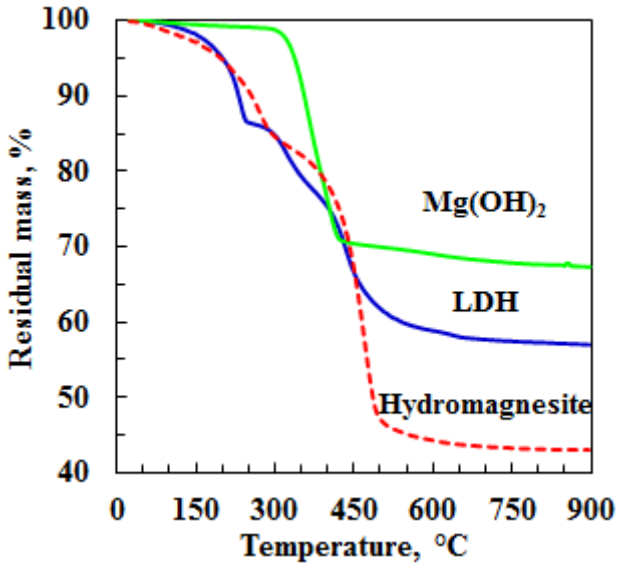

Figure 5. TGA traces for the PVC-LDH composites in (A) nitrogen and (B) air atmospheres. The temperature was scanned from 25 °C to 900 °C at a scan rate of 10 °C min^{-1} with gas flowing at a rate of 50 mL min^{-1}. Key: PVC = no additive; HM= hydromagnesite; MH = magnesium hydroxide, and LDH = layered double hydroxide.

The initial mass loss is due a combination of PVC degradation (mainly dehydrochlorination) events and volatilization of the plasticizer. The second stage is attributed to pyrolysis reactions that ultimately lead to a carbonaceous char residue (4.3 wt. % at 900 °C). The shape of the mass loss curves for the LDH-PVC composite mirrors that of PVC. The mass loss onset temperatures are similar but mass loss occurs over a narrower temperature range and the residue after each stage is greater than found for the neat PVC.

The initial part of the mass loss curves (below 300 °C) found in an air atmosphere is similar to that in a nitrogen atmosphere. However, at higher temperatures additional mass loss occurs owing to the oxidation of the carbonaceous char. The PVC sample residue decreases to zero at ca. 550 °C. The other samples show a greater residue but this represents non-volatile inorganic matter.

Heat stability of the PVC composites

During the primary stage of degradation discoloration of the PVC is observed. It is caused by the formation of conjugated polyene sequences of double bonds along the polymer chain. These defects are highly reactive and they undergo secondary reactions that lead to crosslinking or cleavage of the polymer chains (38). The thermogravimetric analysis performed on the PVC compounds provided basic information on the intrinsic heat stability of the PVC compounds. However, in the present study the progression of PVC degradation was quantified by following the evolution of HCl with the Thermomat method. Representative Thermomat conductivity response curves are shown in Figure 6A. The induction time corresponds to the onset time while the stability time is defined by the time required to reach a conductivity of 50 μS cm^{-1}. The ranking of the stabilisers in terms of the induction times was as follows:

$$\text{LDH} > \text{hydromagnesite} \approx Mg(OH)_2 > \text{neat PVC}$$

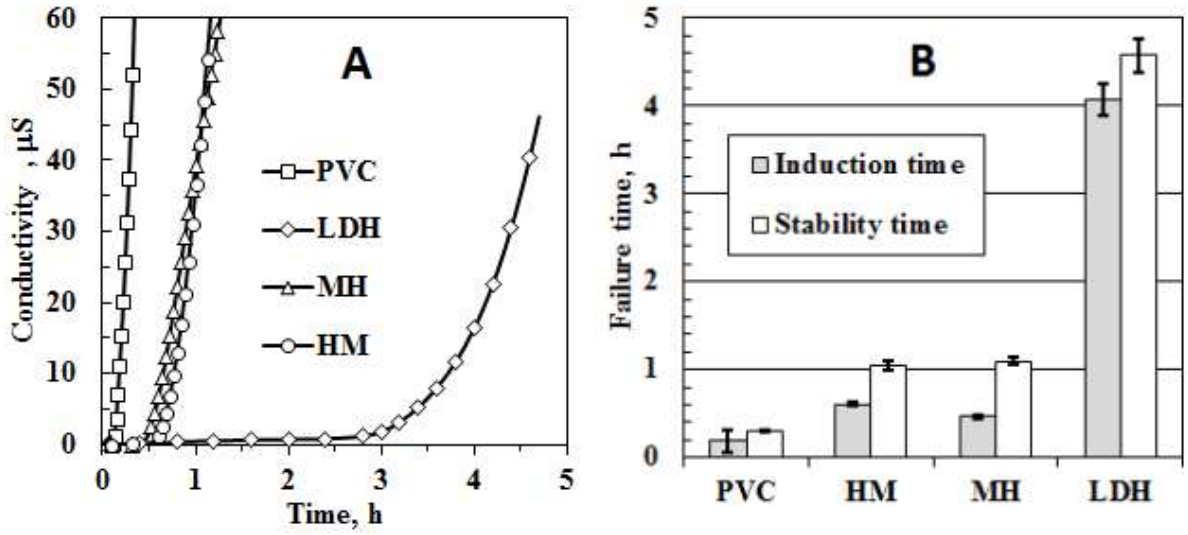

Figure 6. The induction and stability times were obtained by tracking the evolution of hydrochloric acid. A. Representative conductivity curves for the PVC compounds. B. Thermomat static heat stability at 200 °C. Key: PVC = no additive; HM= hydromagnesite; MH = magnesium hydroxide, and LDH = layered double hydroxide.

The effect of the LDH derivatives on the Thermomat stability times of the flexible PVC compounds is shown in the Figure 6B. The neat PVC compound had a stability time of 0.31 ± 0.01 h. Only the LDH provided a significant improvement in both the induction time and the stability time (4.07 ± 0.17 h and 4.57 ± 0.20 h respectively).

PVC degradation and stabilization processes occur via multiple primitive reaction steps, each with their own characteristic temperature-dependent rate constant. In addition, mass transfer effects play a significant role. In view of these complications it is convenient to model the degradation using the single step reaction approximation (39-43). A central feature of PVC degradation is its autocatalytic nature (18, 19). This implies that an autocatalytic reaction mechanism (44, 45) should be considered, e.g.:

$$\frac{d\alpha}{dt} = k\alpha^{1-1/\theta}(1-\alpha)^{1+1/\theta} \qquad (1)$$

where α is the degree of conversion that defines the extent of degradation of the PVC polymer [-]: t is the time [s]; k is the rate constant [s^{-1}] and θ is a dimensionless constant [-]

defining the reaction order. This differential equation provides a parametric interpolation formula between the predictions of the logistic equation ($\theta \to \infty$) describing classic autocatalytic behaviour and second order kinetics ($\theta = 1$). For $1 \le \theta < \infty$ and initial condition $\alpha = 0$ at $t = 0$, the general solution for isothermal conditions is (45):

$$\alpha = 1 - \left[1 + \left(t/\tau\right)^{\theta}\right]^{-1} \qquad (2)$$

Where the time constant is defined by $\tau = \theta/k$.

This equation predicts a rate maximum at a time equal to $\left[\theta/k\right]\left[\left(\theta-1\right)/\theta+1\right]^{1/\theta}$. Furthermore, the predicted S-shaped conversion curve shifts to higher times with increasing θ and lower values for the rate constant *k*. In order to apply equation (2) to the Thermomat data, it was assumed that the conductivity is directly proportional to the degree of degradation of the polymer sample. The parameters τ and θ were then obtained by least squares fitting of Equation (2) to the conductivity *vs.* time curves.

The order parameter for the neat PVC was found to be $\theta = 2.92 \pm 0.12$ and the degradation rate constant was $k = 5.07 \pm 0.26$ h. With LDH as the stabilizer the reaction order parameter was higher ($\theta = 7.06 \pm 0.47$) than that found for the neat PVC. It was also higher for hydromagnesite ($\theta = 5.81 \pm 0.06$ h) while for the magnesium hydroxide it was lower ($\theta = 4.77 \pm 0.15$ h). The LDH stabilizer caused a significant lowering of the degradation rate constant to a value of $k = 1.13 \pm 0.12$ h. However, the deviations, of the rate constants for magnesium hydroxide and hydromagnesite from the value for PVC, were not statistically significant. This means that these additives did not affect the intrinsic rate at which the PVC matrix degraded. The longer induction times that were observed were thus simply due to scavenging of the hydrochloric acid by the basic additives in the initial phase of the PVC degradation.

Table 3. Cone calorimeter data summary

Parameter	**Units**	**PVC**	**LDH**	**$Mg(OH)_2$**	**Hydromagnesite**
Time to ignition (t_{ign})	s	23.0 ± 2.1	27.7 ± 1.2	28.3 ± 1.2	19.3 ± 1.2
Time to flame out	s	306 ± 137	654 ± 51	516 ± 16	527 ± 54
Time to *pHRR*	s	103 ± 10	105 ± 1	98 ± 3	132 ± 6
Peak heat release rate (*pHRR*)	kW m^{-2}	623 ± 8	389 ± 9	419 ± 9	406 ± 12
Total heat release (*tHR*)	MJ m^{-2}	68 ± 2	72 ± 3	74 ± 2	69 ± 3
Effective heat of combustion	MJ kg^{-1}	16.7 ± 0.1	18.2 ± 0.2	16.6 ± 0.4	16.6 ± 0.4
Relative heat of combustion[#]	-	1.00 ± 0.01	1.25 ± 0.01	1.14 ± 0.03	1.14 ± 0.03
FIGRA	kW $m^{-2}s^{-1}$	6.1 ± 0.6	3.7 ± 0.1	4.3 ± 0.2	3.1 ± 0.2
MARHE	kW m^{-2}	367 ± 11	208 ± 2	231 ± 5	252 ± 2
$pHRR/t_{ign}$	kW $m^{-2}s^{-1}$	26.0 ± 0.8	14.4 ± 0.3	14.5 ± 0.3	21.1 ± 1.8
Smoke release	m^2 m^{-2}	4413 ± 97	2780 ± 121	3181 ± 64	3000 ± 101
Char & ash @ 600 °C	wt.%	4.1 ± 0.8	18.4 ± 1.4	15.7 ± 1.7	11.1 ± 0.0

[#]Heat of combustion scaled with respect to PVC plus plasticiser content and relative to the value for the neat PVC compound

Fire testing

The cone calorimeter results are summarized in Table 3 and presented in Figure 7 to Figure 10. All the samples ignited after a short induction period and they all burned producing large amounts of smoke. The time to ignition (t_{ign}) was 23 ± 2 s for the neat PVC compound. It was longer for the $Mg(OH)_2$ and LDH containing compounds but shorter for hydromagnesite (19.3 ± 1.2 s). The TGA results shown in Figure 5 suggest that the hydromagnesite destabilizes the PVC matrix as mass loss commenced at lower temperatures. This may explain the reduced ignition time for this additive. In effect combustible organic fuel residues are released at an earlier time compared to the other compounds. The time to flame out was 306 ± 137 for the neat PVC compound. On average, it increased by 68%, 71% and 114% when $Mg(OH)_2$, hydromagnesite and LDH respectively were added.

Directly after ignition, the neat PVC compound showed rapid mass loss and this was virtually complete by 200 s. Thereafter there was a very slow steady decline in the residue

amount with a char yield of 4.0 wt.% at the end of the test. The filled compounds lost mass at a much slower rate over a longer time. The apparent char yields were 15.9 wt.%, 13.8 wt.% and 11.3 wt.% for the LDH, magnesium hydroxide and hydromagnesite respectively. These values reflect the higher ash content due to the fillers rather than improved carbon yield. It is likely that these ash residues comprise complex mixtures of metal chlorides and oxides.

Figure 7 shows representative heat release rate (*HRR*) curves obtained from the cone calorimeter tests. The heat release curves for the neat plasticised PVC compound exhibited the shape characteristic of a thermally thin sample (46). Thermally thin samples are identified by a sharp peak in their *HRR* curves as the whole sample is pyrolyzed nearly at once. The HRR curves for the filled compounds were flatter and broader than that for the neat PVC. *HRR* curves characteristic of thermally thick, char-producing samples show a sudden rise to a plateau value (46). However, the *HRR* curves for the sample containing hydrated filler were

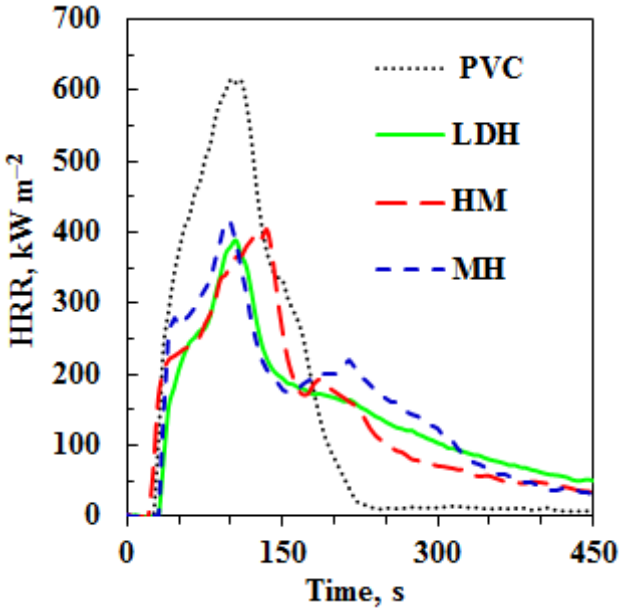

Figure 7. Representative cone calorimeter heat release rate curves for the plasticised PVC compound and its composites with the hydrated fillers. Key: PVC = no additive; HM= hydromagnesite; MH = magnesium hydroxide, and LDH = layered double hydroxide.

more complex. They showed a sudden rise to a peak value with a slow but steady decline over a longer period. The *pHRR* for the neat PVC compound was 623 ± 8 kW m^{-2}. Incorporating LDH derivatives at the 13 wt.% level caused a significant lowering of the *pHRR*. LDH lowered the *pHRR* value to 389 ± 9 kW m^{-2} and the other two additives produced a similar reduction. The CO_2 and CO release rates (not shown graphically) curves mirrored those observed for the *HRR* (Figure 7) almost perfectly.

An important index used to interpret cone calorimeter data is the maximum average rate of heat emission (*MARHE*) (46, 47). The *MARHE* parameter is defined as the peak value of the cumulative heat emission divided by time (47). It provides a measure of the propensity for fire development under full scale conditions. The *MARHE* for the neat PVC was 367 ± 11 kW m^{-2} and this was reduced to 202 ± 2 kW m^{-2} with the LDH as stabiliser-flame retardant. The addition of the other two filler additives also reduced the *MARHE*.

Interesting observations hold for the total heat release (*tHR*) and the effective heat of combustion presented in Table 3. The *tHR* value was 68 ± 2 MJ m^{-2} for the neat PVC compound. With the LDH derivative incorporated, the *tHR* increased even though less fuel is available for combustion. The *tHR* was 72 ± 3 MJ m^{-2} for the LDH compound and the highest value was 74 ± 2 MJ m^{-2} recorded for the magnesium hydroxide. The effective heat of combustion for the PVC was 16.7 ± 0.1 MJ kg^{-1}. Values for the filled compounds were similar or even higher. It is interesting to compare the relative heats of combustion scaled with respect to the organic combustible content of the compounds. These are also presented in Table 3. They show values that are 25% higher for the LDH-filled compound and 14% higher for the other two fillers. Thus while the fire performance improved with respect to the peak heat release rate, it deteriorated when the total heat release (*tHR*) or effective heat of combustion is considered. These apparent increases are tentatively attributed to the chlorine preferentially interacting and reacting with the fillers. Less halogen present in the vapour

phase to inhibit the combustion of the volatile fuel fragments could have resulted in more efficient combustion and hence an increase in the total heat release.

The fire growth rate (*FIGRA*) is an estimator for the fire spread rate and size of the fire (46, 47). The *FIGRA* is defined as the maximum quotient of *HRR*(*t*)/*t*. According to Hirschler (48), the fire performance index (*FPI*) is possibly the best single indicator of the overall fire hazard posed by a material. It is defined as the ratio of the time-to-ignition to the peak heat release rate ($FPI = t_{ign}/pHRR$). There is a connection between *FPI* and the time to flashover, i.e. the change from small to large-scale fire (48). A lower *FPI* value is associated with a shorter time to flashover suggesting that a shorter time is available for escape in a full-scale fire situation. Figure 8 shows the *FIGRA* and *FPI* indices with the latter expressed as it inverse as it then has the same units. Relative to the neat PVC compound, the presence of the LDH markedly decreased the *FIGRA* (>55%). The $pHRR/t_{ign}$ for the neat PVC was 26 ± 1

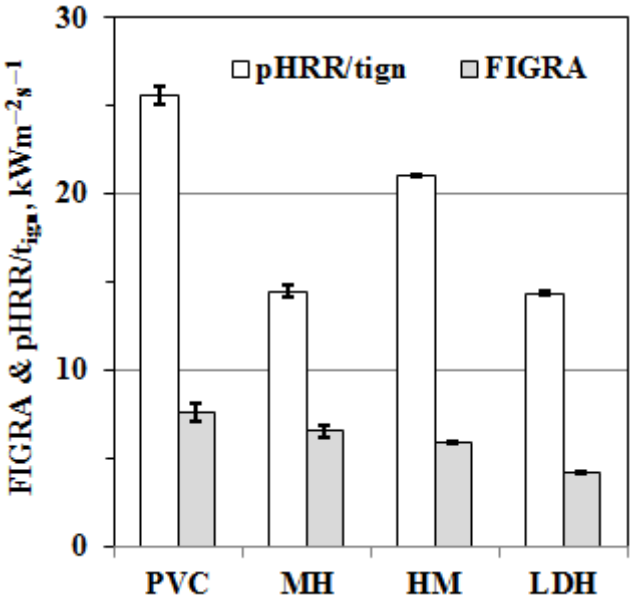

Figure 8. The effect of the hydrated fillers on the *FIGRA* and $pHRR/t_{ign}$ of PVC composites. Key: PVC = no additive; HM= hydromagnesite; MH = magnesium hydroxide, and LDH = layered double hydroxide.

kW $m^{-2}s^{-1}$. It was lowered to 14.4 ± 0.3 kW $m^{-2}s^{-1}$ in the presence of the LDH while the other PVC compounds featured intermediate values.

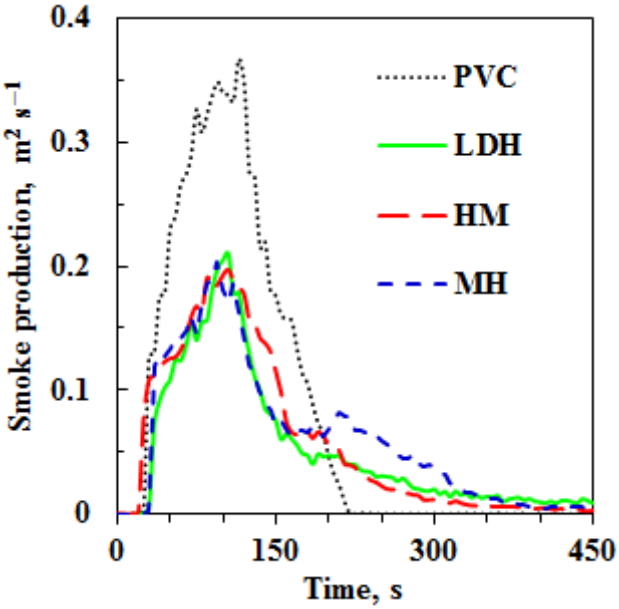

Figure 9. Cone calorimeter smoke production rates for the plasticized PVC compound and its composites with LDH derivatives. Key: PVC = no additive; HM= hydromagnesite; MH = magnesium hydroxide, and LDH = layered double hydroxide.

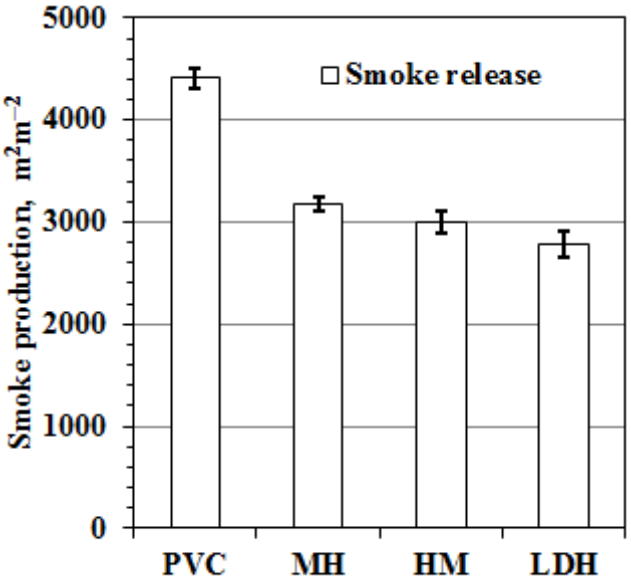

Figure 10. Comparing the smoke production of the plasticized PVC compound with that from its composites with LDH derivatives. Key: PVC = no additive; HM= hydromagnesite; MH = magnesium hydroxide, and LDH = layered double hydroxide.

Figure 9 and Figure 10 show and compare the smoke production rates (*SPR*) and the smoke production of the composites with that for the neat PVC compound. The peak smoke production rate was virtually the same for all the filler additives. However, overall LDH reduced the total smoke production more so than the other hydrated fillers.

Discussion

The performance of the LDH can be explained in the context of the PVC degradation mechanism that occurs in two stages: Crosslinking of the polymer chains and dehydrocarbonation reactions promote char formation (38). Chain cleavage and cracking reactions lead to the formation of volatile aromatic molecules that promote smoke generation. The hydrogen chloride gas generated by the degradation reaction catalyses the chain propagation reaction. The carbonated LDH improves the heat stability of the PVC by scavenging this corrosive gas. Initially this occurs via the formation of chloride intercalated LDH. However, later on the acid attacks the LDH structure leading to the formation of metal chlorides. These salts act as Lewis bases that can also promote dehydrochlorination via a carbonium ion mechanism (8). According to Zhu *et al*. (49) LDH acts as a Lewis acids and induces cationic crosslinking (Friedel–Craft reaction) of neighbouring polyene backbones. Metal chlorides also catalytically favour crosslinking and dehydrocarbonation reactions at the expense of cracking reactions (49). These actions improve char formation and reduce smoke generation in accordance with the present experimental results.

The release of the HCl by the decomposing PVC inhibits flaming combustion in the cone calorimeter tests. The halogen entering the gas phase contributes to a "flame poisoning effect", i.e. the slowing down of the free radical chain reactions occurring in the flame (9). In the presence of the LDH, the HCl is efficiently scavenged especially in the early stages of degradation. Less halogen is present in the volatile organics released in the beginning making

them easier to ignite. This may help explain the shorter time to ignition found for the hydromagnesite compound compared to neat PVC.

The superior fire performance obtained with the LDH, compared to magnesium hydroxide, was previously observed in another polymer matrix, i.e. EVA (50). Compared to the neat PVC, all the filler additives decreased the peak heat release rate in the cone calorimeter tests. This may be due to a combination of vapour phase and solid phase effects. High heat decomposes the fillers releasing water or water and carbon dioxide. The decomposition is endothermic in nature which means that it cools the polymer substrate. At lower temperature the degradation reactions that generate fuel proceeds more slowly. This explains in part the rate of lower mass loss observed for the LDH compound in the cone calorimeter tests. In addition the inert gases liberated have a dilution effect on the air-fuel mixture in the gas phase. This cools the flame reducing the rate of heat generation. The inorganic residues may form a protective layer on the surface of the substrate. It may act as a barrier to heat transfer to the underlying polymer and also to mass transfer of degradation products migrating to the gas phase. Finally the inorganic residues may effectively reflect incoming infrared radiation that would otherwise have heated the substrate to higher temperatures. All these effects may contribute to the lowering of the heat release rate observed in the cone calorimeter tests.

Finally, at elevated temperature and in the presence of oxygen, the metal oxide residues from the decomposition of the LDH catalyse the oxidation of the carbonaceous char residues. This explains the absence of organic residues above 600 °C in the TGA runs conducted in an air atmosphere.

Conclusion

Layered double hydroxide (LDH) [$Mg_4Al_2(OH)_{12}CO_3.4H_2O$] and hydromagnesite [$4MgCO_3.Mg(OH)_2{\cdot}4H_2O$] (HM) flame retardant fillers were successfully synthesised using hydrothermal methods. Characterisation using XRD, ICP-MS and FTIR confirmed that the products approached these idealised compositions.

Emulsion grade PVC was plasticized with 100 phr of diisononyl phthalate and filled with 30 phr layered double hydroxide (LDH), hydromagnesite or magnesium hydroxide as combination stabilizer-flame retardant additives. It was found that LDH showed good performance in a static heat stability test. Analysis of the Thermomat data suggests that this additive actually modifies the PVC degradation mechanism. The hydromagnesite and magnesium hydroxide improved heat stability too but only marginally. Analysis of the Thermomat data suggests that, unlike the LDH, these basic additives did not affect the intrinsic rate at which the PVC matrix degraded. They retarded the degradation process primarily by scavenging the hydrochloric acid liberated during the initial phase of the PVC degradation. The LDH filler performed better than magnesium hydroxide and hydromagnesite with respect to most fire retardant performance indices e.g. the fire growth rate (FIGRA) the maximum average rate of heat emission (MARHE) and the fire performance index (FPI). It lowered the peak heat release rate (*pHRR*), from 623 ± 8 kW m^{-2} to 389 ± 9 kW m^{-2} but increased the total heat release from 68 ± 2 MJ m^{-2} to only 72 ± 3 MJ m^{-2}. The LDH filler was also more effective at reducing the total smoke production. It is concluded that LDH is a promising functional filler for plasticized PVC that imparts both heat stability and improved fire performance.

References

1. Miyata S, Kumura T. Synthesis of new hydrotalcite-like compounds and their physico-chemical properties. Chemistry Letters. 1973;2(8):843-8.
2. Sato T, Fujita H, Endo T, Shimada M, Tsunashima A. Synthesis of hydrotalcite-like compounds and their physico-chemical properties. Reactivity of Solids. 1988;5(2–3):219-28.
3. Bellotto M, Rebours B, Clause O, Lynch J, Bazin D, Elkaïm E. A Reexamination of Hydrotalcite Crystal Chemistry. The Journal of Physical Chemistry. 1996;100(20):8527-34.
4. White WB. Infrared characterization of water and hydroxyl ion in the basic magnesium carbonate minerals. American Mineralogist. 1971;56:46-53.
5. Coaker AW. Fire and flame retardants for PVC. Journal of Vinyl and Additive Technology. 2003;9(3):108-15.
6. Otani S. On the carbon fiber from the molten pyrolysis products. Carbon. 1965;3(1):31-8.
7. Folarin OM, Sadiku ER. Thermal stabilizers for poly(vinyl chloride): A review. International Journal of Physical Sciences. 2011;6(18):4323-30.
8. Levchik SV, Weil ED. Overview of the recent literature on flame retardancy and smoke suppression in PVC. Polymers for Advanced Technologies. 2005;16(10):707-16.
9. Weil ED, Levchik S, Moy P. Flame and smoke retardants in vinyl chloride polymers - Commercial usage and current developments. Journal of Fire Sciences. 2006;24(3):211-36.
10. Hornsby PR. The application of hydrated mineral fillers as fire retardant and smoke suppressing additives for polymers. Macromolecular Symposia. 1996;108(1):203-19.

11. Hornsby PR. Fire retardant fillers for polymers. International Materials Reviews. 2001;46(4):199-210.
12. Xu ZP, Saha SK, Braterman PS, D'Souza N. The effect of Zn, Al layered double hydroxide on thermal decomposition of poly(vinyl chloride). Polymer Degradation and Stability. 2006;91(12):3237-44.
13. Wang X, Zhang Q. Effect of hydrotalcite on the thermal stability, mechanical properties, rheology and flame retardance of poly(vinyl chloride). Polymer International. 2004;53(6):698-707.
14. Gao Y, Wu J, Wang Q, Wilkie CA, O'Hare D. Flame retardant polymer/layered double hydroxide nanocomposites. Journal of Materials Chemistry A. 2014;2(29):10996-1016.
15. Hornsby PR, Watson CL. A study of the mechanism of flame retardance and smoke suppression in polymers filled with magnesium hydroxide. Polymer Degradation and Stability. 1990;30(1):73-87.
16. Laoutid F, Bonnaud L, Alexandre M, Lopez-Cuesta JM, Dubois P. New prospects in flame retardant polymer materials: From fundamentals to nanocomposites. Materials Science and Engineering: R: Reports. 2009;63(3):100-25.
17. Braun D. Poly(vinyl chloride) on the Way from the 19th Century to the 21st Century. Journal of Polymer Science, Part A: Polymer Chemistry. 2004;42(3):578-86.
18. Starnes Jr WH, Ge X. Mechanism of autocatalysis in the thermal dehydrochlorination of poly(vinyl chloride). Macromolecules. 2004;37(2):352-9.
19. Starnes Jr WH. Structural and mechanistic aspects of the thermal degradation of poly(vinyl chloride). Progress in Polymer Science (Oxford). 2002;27(10):2133-70.
20. Lin Y-J, Li D-Q, Evans DG, Duan X. Modulating effect of Mg–Al–CO3 layered double hydroxides on the thermal stability of PVC resin. Polymer Degradation and Stability. 2005;88(2):286-93.

21. van der Ven L, van Gemert MLM, Batenburg LF, Keern JJ, Gielgens LH, Koster TPM, et al. On the action of hydrotalcite-like clay materials as stabilizers in polyvinylchloride. Applied Clay Science. 2000;17(1–2):25-34.
22. Lin Y, Wang J, Evans DG, Li D. Layered and intercalated hydrotalcite-like materials as thermal stabilizers in PVC resin. Journal of Physics and Chemistry of Solids. 2006;67(5-6):998-1001.
23. Gupta S, Agarwal DD, Banerjee S. Role of hydrotalcites cations in thermal stabilization of poly (vinyl chloride). International Journal of Polymeric Materials and Polymeric Biomaterials. 2012;61(2):124-35.
24. Miyata S, Kuroda M. Method for inhibiting the thermal or ultraviolet degradation of thermoplastic resin and thermoplastic resin composition having stability to thermal or ultraviolet degradation. US Patent 4,299,759; 1981.
25. Labuschagné FJWJ, Giesekke EW, Van Schalkwyk JD, inventors SA Patent 2007/09947 Production of hydrotalcite. South Africa2007.
26. ISO. Plastics - Determination of the tendency of compounds and products based on vinyl chloride homopolymers and copolymers to evolve hydrogen chloride and any other acidic products at elevated temperatures Part 3: Conductometric method1993.
27. ISO. ISO/TS 5660-3:2012 Reaction-to-fire tests - Heat release, smoke production and mass loss rate. Part 3: Guidance on measurement. Geneva: ISO; 2012.
28. ISO. ISO 5660-2:2002 Reaction-to-fire tests - Heat release, smoke production and mass loss rate. Part 2: Smoke production rate (dynamic measurement). Geneva: ISO; 2002.
29. ISO. ISO 5660-1:2015 Reaction-to-fire tests - Heat release, smoke production and mass loss rate. Part 1: Heat release rate (cone calorimeter method) and smoke production rate (dynamic measurement). Geneva: ISO; 2015.

30. Wang Z, Huang, P., Fan, W.C., Wang, Q., editor Measurements on the fire behaviour of PVC sheets using the cone calorimeter. Proceedings of the Asia-Oceania Symposium on Fire Science & Technology; 1988: International Association for Fire Safety Science.
31. Kloprogge JT, Wharton D, Hickey L, Frost RL. Infrared and Raman study of interlayer anions CO32−, NO3−, SO42− and ClO4− in Mg/Al-hydrotalcite. American Mineralogist. 2002;87(5-6):623-9.
32. Choudhary VR, Pataskar SG, Gunjikar VG, Zope GB. Influence of preparation conditions of basic magnesium carbonate on its thermal analysis. Thermochimica Acta. 1994;232(1):95-110.
33. Sawada Y, Yamaguchi J, Sakurai O, Uematsu K, Mizutani N, Kato M. Thermogravimetric study on the decomposition of hydromagnesite 4 MgCO3 · Mg(OH)2 · 4 H2O. Thermochimica Acta. 1979;33(C):127-40.
34. Ren H, Chen Z, Wu Y, Yang M, Chen J, Hu H, et al. Thermal characterization and kinetic analysis of nesquehonite, hydromagnesite, and brucite, using TG-DTG and DSC techniques. Journal of Thermal Analysis and Calorimetry. 2014;115(2):1949-60.
35. Vágvölgyi V, Frost RL, Hales M, Locke A, Kristóf J, Horváth E. Controlled rate thermal analysis of hydromagnesite. Journal of Thermal Analysis and Calorimetry. 2008;92(3):893-7.
36. Rey F, Fornes V, Rojo JM. Thermal decomposition of hydrotalcites. An infrared and nuclear magnetic resonance spectroscopic study. Journal of the Chemical Society, Faraday Transactions. 1992;88(15):2233-8.
37. Bera P, Rajamathi M, Hegde MS, Kamath PV. Thermal behaviour of hydroxides, hydroxysalts and hydrotalcites. Bull Mater Sci. 2000;23(2):141-5.
38. Bacaloglu R, Stewen U. Study of PVC degradation using a fast computer scanning procedure. Journal of Vinyl and Additive Technology. 2001;7(3):149-55.

39. Malík J, Kröhnke C. Polymer stabilization: present status and possible future trends. Comptes Rendus Chimie. 2006;9(11–12):1330-7.
40. Šimon P. Considerations on the single-step kinetics approximation. Journal of Thermal Analysis and Calorimetry. 2005;82(3):651-7.
41. Dente M, Bozzano G, Faravelli T, Marongiu A, Pierucci S, Ranzi E. Kinetic Modelling of Pyrolysis Processes in Gas and Condensed Phase. In: Guy BM, editor. Advances in Chemical Engineering. Volume 32: Academic Press; 2007. p. 51-166.
42. Anderson HL, Kemmler A, Höhne GWH, Heldt K, Strey R. Round robin test on the kinetic evaluation of a complex solid state reaction from 13 European laboratories. Part 1. Kinetic TG-analysis. Thermochimica Acta. 1999;332(1):33-53.
43. Pospíšil J, Horák Z, Pilař J, Billingham NC, Zweifel H, Nešpůrek S. Influence of testing conditions on the performance and durability of polymer stabilisers in thermal oxidation. Polymer Degradation and Stability. 2003;82(2):145-62.
44. Kamal MR, Sourour S. Kinetics and thermal characterization of thermoset cure. Polymer Engineering & Science. 1973;13(1):59-64.
45. Labuschagne F, Molefe DM, Focke WW, van der Westhuizen I, Wright HC, Royeppen MD. Heat stabilising flexible PVC with layered double hydroxide derivatives. Polymer Degradation and Stability. 2015;113:46–54.
46. Schartel B, Hull TR. Development of fire-retarded materials—Interpretation of cone calorimeter data. Fire and Materials. 2007;31(5):327-54.
47. Sacristán M, Hull TR, Stec AA, Ronda JC, Galià M, Cádiz V. Cone calorimetry studies of fire retardant soybean-oil-based copolymers containing silicon or boron: Comparison of additive and reactive approaches. Polymer Degradation and Stability. 2010;95(7):1269-74.

48. Hirschler MMS, S., editor. Flame Retardants 92; 1992; London/New York: Elsevier Applied Science.
49. Zhu H, Wang W, Liu T. Effects of copper-containing layered double hydroxide on thermal and smoke behavior of poly(vinyl chloride). Journal of Applied Polymer Science. 2011;122(1):273-81.
50. Camino G, Maffezzoli A, Braglia M, De Lazzaro M, Zammarano M. Effect of hydroxides and hydroxycarbonate structure on fire retardant effectiveness and mechanical properties in ethylene-vinyl acetate copolymer. Polymer Degradation and Stability. 2001;74(3):457-64.

Wang, Z., Huang, P., Fan, W.C. and Wang, Q. Measurements on the fire behaviour of PVC sheets using the cone calorimeter. *Proceedings of the Asia-Oceania Symposium on Fire Science & Technology* (*AOFST* 3), National University of Singapore, Singapore, June 10-12, 1998: International Association for Fire Safety Science. http://www.iafss.org/publications/aofst/3/221#

Hirschler, M. M. and Shakir, S., in *Proceedings from Flame Retardants 92.* Elsevier Applied Science, London-/New York, 1992. p. 77.